Nuclear Radii by Scattering of Low-Energy Neutrons*

K. K. SETH,† D. J. HUGHES, R. L. ZIMMERMAN, AND R. C. GARTH‡
Brookhaven National Laboratory, Upton, New York

(Received January 16, 1958)

The potential scattering cross section for slow neutrons, σ_p, has been measured for seventeen elements in order to determine the nuclear potential radius and to investigate the predictions of nuclear optical models. The measurements were based on total cross sections resulting from transmission experiments performed with the Brookhaven fast chopper. In the energy region where individual resonances can be resolved and their parameters determined with reasonable accuracy, σ_p is obtained by subtracting the resonance contribution, including interference effects, from the measured total cross section. In the kev region, where the chopper resolution permits determination of cross sections averaged over many resonances only, different sample thicknesses are used and σ_p derived from the slope of the transmission curve. The results in the two energy regions agree, thereby justifying the concept of potential scattering as a cross section constant with energy, once effects of nearby resonances are removed. The variation of potential scattering with atomic weight is compared with predictions of optical models of the nucleus. The data reflect rather strongly the effects of the deformation of the nuclear shape from spherical, and good agreement is obtained for a potential well with a diffuse surface and nuclear deformations corresponding to known quadrupole moments. The radius of the potential (the distance to its half-value) is given by $R=r_0A^{\frac{1}{3}}$, with $r_0=(1.35\pm0.04)\times10^{-13}$ cm. The radius parameter r_0 is thus distinctly larger than the 1.09×10^{-13} cm obtained from electron scattering experiments.

I. INTRODUCTION

THE use of neutron, proton, or alpha-particle scattering experiments to give information on nuclear radii is not as straightforward as electron scattering, because of the still rather poorly understood nature of nuclear forces. As a result, all conclusions concerning nuclear size and shape resulting from such experiments are more or less model-dependent. Thus the scattering of protons of several Mev energy gives the quantity VR^2, where V is the well depth, rather than the nuclear radius R itself.[1] Other experimental results, or a well depth computed from some model, must be utilized to obtain R from the proton scattering. In the present paper we report measurements of the potential scattering, σ_p, of low-energy neutrons, a quantity that is reasonably directly related to the nuclear potential radius rather than the quantity VR^2. The experimental problem of extracting σ_p from the total cross section requires careful analysis but the results can be interpreted in terms of R with little dependence on the well depth.

As R is the radius of the nuclear potential well that is appropriate for the particular bombarding particle, care must be taken in its definition if it is to be independent of the nature, charge, and energy of the particle used in its investigation. Various experiments measure different moments of the radial potential distribution, and in the analysis different shapes for the distribution are often used. It thus is often necessary to define equivalent radii that can be directly compared, such as an equivalent radius defined as that of a uniform (square) distribution that will reproduce the features of the actual distribution employed. For the measurements reported in this paper we shall take the radius R to be the distance at which the potential attains half its central value.

The optical model of the nucleus, which is the usual means for interpreting scattering experiments, is a compromise between the independent-particle and the compound-nucleus models. In their adaptation of this model to low-energy neutron scattering Feshbach, Porter, and Weisskopf[2] used a potential well that has a real (elastic scattering) and an imaginary (compound nucleus formation) part,

$$\begin{aligned} V&=-V_0(1+i\zeta) \quad \text{for } r<R, \\ V&=0 \qquad\qquad\ \ \text{for } r>R, \end{aligned} \tag{1}$$

where $R=r_0A^{\frac{1}{3}}$ and ζ is the ratio of the imaginary to the real component of the potential.

On the basis of this model they define the elastic scattering as made up of "shape elastic" plus "compound elastic" scattering. We shall use the more customary "potential scattering" for the former, even though it has often been applied rather vaguely. The potential scattering is the analog of hard-sphere scattering, resulting from the nonpenetrability of the nucleus to neutrons of nonresonant energies. For s-wave neutrons its cross section is given by

$$\sigma_p=4\pi(R')^2, \tag{2}$$

where R' is a length of the order of the nuclear radius R. The compound elastic scattering is the part of elastic scattering that results from formation of a compound nucleus and re-emission of a neutron into the entrance channel. Between resonances the elastic cross section is mainly potential scattering and at resonances mainly compound elastic scattering. Because of the interference of these components, their separation in practice is difficult, as we shall see.

It can be shown that Eq. (2) has some very interest-

* Work performed under contract with U. S. Atomic Energy Commission.

† Now at Duke University, Durham, North Carolina.

‡ Permanent address: Brooklyn College, Brooklyn, New York.

[1] Glassgold, Cheston, Stein, Schuldt, and Erickson, Phys. Rev. **106**, 1207 (1957); A. E. Glassgold and P. J. Kellogg, Phys. Rev. **109**, 1291 (1958).

[2] Feshbach, Porter, and Weisskopf, Phys. Rev. **96**, 448 (1954).

ing properties at the points $(R'/R)=1$, where, for the potential of Eq. (1),

$$K_0R=\left(\frac{2m}{\hbar^2}V_0R^2\right)^{\frac{1}{2}}=\tfrac{1}{2}n\pi, \tag{3}$$

with n an integer, and K_0 and m the wave number in the well and mass of the neutron. The points where $R=R'$ are determined by the product V_0R^2, which is well determined by strength function measurements for low-energy neutrons. At these points a measured value of R' gives R with no corrections and at other atomic weights R' differs somewhat from R but the dependence on the model parameters is usually not great. It is because of the weak dependence on model parameters that the potential scattering at low energy is a useful method for obtaining R independently of V.

Feshbach, Porter, and Weisskopf[3] have recently carried out calculations of low-energy neutron scattering for a rounded potential well of the form

$$V(r)=-V_0\frac{(1+i\zeta)}{1+\exp[2(r-R)/d]}, \tag{4}$$

with the following parameters:

$$\begin{aligned} &V_0=42\text{ Mev},\quad \zeta=0.08,\quad K_0d=1.65,\\ &R=r_0A^{\frac{1}{3}},\quad \text{with } r_0=1.35\times10^{-13}\text{ cm}. \end{aligned} \tag{5}$$

The shape of the imaginary potential was kept the same as that of the real part, mostly for convenience in calculation, and the nuclei were assumed spherical. The results are in general similar to those for the square well but some quantitative differences exist, the rounded-well results giving closer agreement with experiment than the square well.

The fact that some nuclei are deformed from their spherical shape is expected to affect the predicted scattering and is important to consider, particularly for comparison with accurate experimental results. A qualitative investigation of the effect of constant deformations on the strength function and (R'/R) has been made by Margolis and Troubetzkoy.[4] Chase, Wilets, and Edmonds[5] have calculated the strength function and R' for the optical model, using the actual measured nuclear deformations. The experimental results reported in the present paper will be compared with the latter calculations, as well as with those of Feshbach, Porter, and Weisskopf. The experimental values of σ_p give R' immediately, through Eq. (2), and use of the calculations of the optical model then gives R.

[3] Feshbach, Porter, and Weisskopf (unpublished); reported by V. F. Weisskopf, in Physica **18**, 952 (1956).
[4] B. Margolis and E. S. Troubetzkoy, Phys. Rev. **106**, 105 (1957).
[5] Chase, Wilets, and Edmonds, Phys. Rev. (to be published).

II. EXPERIMENTAL METHOD

The results reported in this paper are based on total cross sections, resulting from transmission measurements performed with the Brookhaven fast chopper.[6-8] Changes in the design of the chopper[8] to enable it to attenuate γ rays more effectively, as well as development[9] of detectors, have been described before. A new 1024-channel time-of-flight analyzer, designed by M. Graham of Brookhaven National Laboratory, is now in use. It uses 16 cathode-ray tubes for memory, and a cathode-ray tube for analog display. At the end of an experimental run, the data stored in the memory, which are displayed on the analog, can be printed out on a teletype machine or plotted directly as a curve of counting rate *vs* flight time. In the present work, the use of thick samples, hence low transmissions, to insure good accuracy in absolute cross sections, required the use of short cycling procedures in order to normalize transmission measurements made over long periods of time.

The observed total cross section consists of a rather involved combination of potential scattering, resonance scattering, and resonance absorption. In order to obtain the potential scattering and hence R', it is necessary to separate it from the resonance contribution. Because of the interference of potential with resonance scattering, the separation requires careful consideration of the interference effects. In addition it is necessary to investigate the validity of the potential-scattering concept, i.e., that subtraction of the contributions of a number of nearby resonances will produce a residual cross section, the potential scattering, that is constant with energy.

The partial cross sections for absorption and scattering at energy E, resulting only from a single resonance at energy E_0 and potential scattering, are given by

$$\sigma_{\text{abs}}=\frac{4\pi\lambda\!\!\!^{-}_0{}^2g\Gamma_n\Gamma_\gamma(E_0/E)^{\frac{1}{2}}}{4(E-E_0)^2+\Gamma^2}, \tag{6}$$

$$\sigma_{\text{sc}}=4\pi g\left|\frac{\lambda\!\!\!^{-}_0\Gamma_n/2}{(E-E_0)+i\Gamma/2}+R'\right|^2+4\pi(1-g)(R')^2. \tag{7}$$

Here $\lambda\!\!\!^{-}_0=1/(2\pi)$ times the neutron wavelength at energy E_0, the Γ's are widths expressed as values at E_0, and

$$g=\tfrac{1}{2}\left(1\pm\frac{1}{2I+1}\right), \tag{8}$$

for $l=0$ (s-wave neutrons). If we denote the two

[6] F. G. P. Seidl, Brookhaven National Laboratory Report 278 (T.46), 1954 (unpublished).
[7] Seidl, Hughes, Palevsky, Levin, Kato, and Sjöstrand, Phys. Rev. **95**, 476 (1954).
[8] Seidl, Palevsky, Hughes, and Zimmerman, J. Nuclear Instr. **1**, 92 (1957).
[9] Muether, Palevsky, and Zimmerman, Bull. Am. Phys. Soc. Ser. II, **2**, 217 (1957).

possible values of g for $J=I\pm\frac{1}{2}$ by g_1 and g_2, we can express the total cross section, including contributions from all levels, as

$$\sigma_t=\sigma_{\rm abs}+\sigma_{\rm sc}=\sum_{E_{01}}\frac{4\pi\lambda_0^2 g_1\Gamma_n\Gamma_\gamma(E_0/E)^{\frac{1}{2}}}{4(E-E_0)^2+\Gamma^2}+\sum_{E_{02}}\frac{4\pi\lambda_0^2 g_2\Gamma_n\Gamma_\gamma(E_0/E)^{\frac{1}{2}}}{4(E-E_0)^2+\Gamma^2}+4\pi g_1\left|\sum_{E_{01}}\frac{\lambda_0\Gamma_n/2}{(E-E_0)+i\Gamma/2}+R'\right|^2+4\pi g_2\left|\sum_{E_{02}}\frac{\lambda_0\Gamma_n/2}{(E-E_0)+i\Gamma/2}+R'\right|^2, \quad (9)$$

where the summation E_{01} is taken over all resonances with $g_1=\frac{1}{2}[1+1/(2I+1)]$, and E_{02} is taken over all resonances with $g_2=\frac{1}{2}[1-1/(2I+1)]$.

Equation (9) is the correct multilevel formula that expresses σ_t at any energy, including the coherent addition of amplitudes for levels of a single spin. However, it cannot be used as such, because of lack of knowledge of the J values of most of the resonances involved, which makes it impossible to assign them to either of the summations correctly. Of course for target nuclides of zero spin only one spin state is possible and Eq. (9) can be directly used, but for most nuclides Eq. (9) cannot be used and an approximation must be utilized in obtaining R' from the experiments. In the present work, the procedure we have used consists of calculating the cross section individually for each resonance and then adding the results algebraically to get the total cross section. This procedure corresponds approximately to Eq. (9), with the modification that the resonance-resonance interference, which is automatically taken into account in Eq. (9), is neglected. The resonance-potential interference is of course included. An estimate of the resonance-resonance effect shows that it is usually negligibly small ($\sim$0.01 barn).

A convenient expression for the difference between the total and potential cross section obtained by this procedure is

$$\sigma_r=\sigma_t-4\pi(R')^2=\sum_{E_0}\frac{(0.6509\times10^6)g\Gamma_n^0}{(E-E_0)+\Gamma^2/4}\times\left[\Gamma_n^0+\frac{\Gamma_\gamma}{\sqrt{E}}+0.879R'(E-E_0)\right], \quad (10)$$

where E, E_0, Γ, Γ_n^0 (the neutron width at 1 ev$=\Gamma_n/\sqrt{E_0}$), and Γ_γ are in ev, and R' is in units of 10^{-13} cm. The cross section σ_r is the amount that must be subtracted from σ_t to obtain the potential scattering $4\pi(R')^2$.

Two energy regions were used to obtain the potential scattering; low energy, where individual resonances could be clearly resolved, and "high" energy (kev region), where only the cross section averaged over resonances was observed. In the former region, where most of the measurements were made, Eq. (10) was applied between the resonances, and in the latter a thick-sample procedure was used to eliminate the resonance contribution experimentally.

A. Between-Resonances Method

This method is applied in the energy region, typically below 1 kev, where individual resonances can be clearly resolved and their parameters measured. For most of the nuclei investigated, the parameters for the significant resonances were available from the extensive tabulation in BNL-325 and its supplement.[10] For the few cases where resonances had not been analyzed, a determination of their parameters was made by the usual methods of area analysis.[11]

From the known resonance parameters, σ_r is calculated as a function of energy from Eq. (10) for all the known contributing resonances, and subtracted from the experimental σ_t. The resulting cross section in many cases is remarkably constant with energy as is shown in Fig. 1 for uranium, for example. The constancy of $\sigma_t-\sigma_r$ with energy as well as the agreement of its numerical value with the result of the measurements in the kev energy region, justifies the identification with potential scattering.

For some elements, however, $\sigma_t-\sigma_r$ is not constant, especially at low energy, and it is necessary to investigate possible contributions of unknown levels at great distances, or more likely, nearby negative-energy levels, that is, bound levels of the compound nucleus.

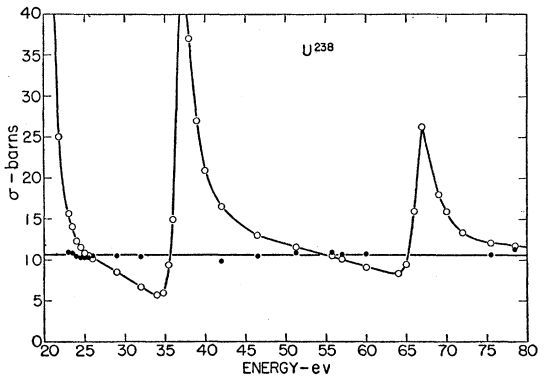

FIG. 1. The determination of the potential scattering for uranium by the between-resonances method. The open circles are the measured total cross sections and the solid points are obtained by correcting for the effect of resonances.

[10] D. J. Hughes and J. A. Harvey, *Neutron Cross Sections*, Brookhaven National Laboratory Report BNL-325 (Superintendent of Documents, U. S. Government Printing Office, Washington 25, D. C., 1955); D. J. Hughes and R. B. Schwartz, *Neutron Cross Sections*, Brookhaven National Laboratory Report BNL-325, Supplement No. 1 (Superintendent of Documents, U. S. Government Printing Office, Washington 25, D. C., 1957).

[11] D. J. Hughes, J. Nuclear Energy **1**, 237 (1955).

If it is assumed that the interference term contributions, the term involving R' in Eq. (10), arising from distant negative- and positive-energy resonances are equal and opposite and therefore cancel out, the remaining effect of such levels on σ_t can be evaluated as an integral over the first two terms in Eq. (10). This integral can be easily evaluated, in terms of average level properties, and under the assumption that $E_0 \gg E$ or $E_0 \gg \Gamma$, leads to a particularly simple answer for the contribution to σ_r from distant positive and negative energy levels,

$$\Delta\sigma_r = 0.6509\times 10^6(\bar{\Gamma}_n^0/D)(\bar{\Gamma}_n^0+\Gamma_\gamma/\sqrt{E})1/\sqrt{E_1}. \quad (11)$$

Here all quantities are in ev, E_1 is the positive energy up to which individual resonances have been taken into account in Eq. (10), $\bar{\Gamma}_n^0$ is the average reduced neutron width, and D is the average level spacing per spin state. It can be shown that, even in the extreme cases, like Pb^{207}, where both $\bar{\Gamma}_n^0$ and Γ_γ are large, the contribution from distant levels, $\Delta\sigma_r$, is negligibly small ($\simeq$0.002 barn).

The cross section σ_r calculated from Eqs. (10) and (11) takes into account the effect of individual levels between energies 0 and E_1, and the integrated contribution of levels beyond $+E_1$ and $-E_1$. It remains to consider possible levels in the interval $-E_1$ to 0. The presence of such levels is indicated by the nonconstancy of $(\sigma_t-\sigma_r)$ near zero energy, as shown in Fig. 2 for Th, for example, as well as by a discrepancy between the measured value of the thermal absorption cross section relative to that calculated from the contribution of the known resonances at low energy. The behavior of $(\sigma_t-\sigma_r)$ near zero energy and the thermal absorption often give sufficient information to compute the properties of the important negative energy levels.

The contributions to the thermal absorption cross section of the known positive-energy resonances and the positive and negative energy levels beyond E_1 are given by

$$\sigma_{abs} = \sum_{E_0=0}^{E_1} \frac{4.119\times 10^6\Gamma_\gamma g\Gamma_n^0}{(0.0253-E_0)^2+\Gamma^2/4} + 4.119\times 10^6\Gamma_\gamma(\bar{\Gamma}_n^0/D)1/E_1, \quad (12)$$

where all parameters are in ev, and the second term is the estimated effect of the levels more distant than E_1. The difference between the measured and calculated absorption is attributed to negative-energy resonances in the region 0 to $-E_1$ ev, which could be expressed similarly to the summation in Eq. (12) if the individual level parameters were known. Usually an attempt is made to explain the difference in terms of a single predominant negative energy level, which can also account for the energy variation of $\sigma_t-\sigma_r$. This method of investigating negative energy levels will now be illustrated by two typical examples.

Gold.—From BNL-325, we have $\sigma_{abs}=98.0+1.0$ barns, $\Gamma_\gamma=0.125$ ev, and the strength function $\bar{\Gamma}_n^0/D=(0.8\pm0.2)\times10^{-4}$. Using Eq. (12), we calculate the contribution to σ_{abs} of all individual levels listed in BNL-325 up to 200 ev as 97.1±3 barns, and of levels beyond this energy as 0.2 barn. Thus we have a calculated cross section of 97.3±3 barns compared with the measured 98.0±1.0 barns, showing that no negative energy level need be invoked to account for the thermal cross section. This does not mean that there are no levels between 0 and $-E_1$, but only that they are small enough not to affect σ_{abs}, hence certainly not σ_t in the region of energy in which we are interested.

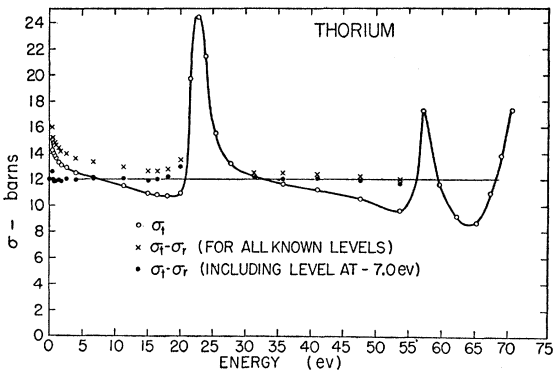

FIG. 2. The determination of the potential scattering for thorium by the between-resonances method. The $\sigma_t-\sigma_r$ obtained by correction for known levels is not constant but inclusion of a level at −7.0 ev produces a constant cross section, which is taken as the potential scattering.

Thorium.—Harvey and Schwartz[12] give $\sigma_{abs}=7.45\pm0.15$ barns, $\Gamma_\gamma=0.030\pm0.010$ ev, $\bar{\Gamma}_n^0/D=(1.0\pm0.2)\times10^{-4}$, and $\bar{\Gamma}_n^0=(1.5\pm0.6)\times10^{-3}$ ev. The contribution of all known levels up to $E_1=70$ ev is equal to 0.355 ±0.19 barn, and the total calculated σ_{abs} is 0.775±0.27 barn. The unaccounted thermal absorption is thus 6.67±0.43 barns, in great contrast to the case of gold. A single negative energy level must have $\Gamma_n^0/E_0^2=0.0540\pm0.02$ to supply the missing absorption. A large number of combinations of Γ_n^0 and E_0 are possible, but of these only a level at $E_0=-7.0$ ev with $\Gamma_n^0=0.0055$ ev produces a constant $(\sigma_t-\sigma_r)$, shown in Fig. 2. This is the single level that removes the discrepancy in σ_{abs} and $(\sigma_t-\sigma_r)$. Although in actuality there may be more than one negative energy level, the net effect is the same as for the single level.

The examples of gold and thorium illustrate the manner in which corrections were applied to the total cross sections between resonances in order to get σ_p. Seventeen elements were investigated in this way and their results are presented in Sec. III. For most cases, the magnitude of the corrections for negative energy levels was negligibly small. Where their contribution was significant, however, larger errors in σ_p indicate the uncertainty resulting from such levels.

[12] J. A. Harvey and R. B. Schwartz, in *Progress in Nuclear Energy, Physics and Mathematics*, edited by D. J. Hughes and J. Sanders (Pergamon Press, London, 1958), Vol. 2.

B. Average-Cross-Section Method

In the kev region, the instrumental resolution of the fast chopper is insufficient to resolve individual resonances, especially in heavy nuclei where the average level spacing is of the order of a few ev. Rather the average cross section is observed, which depends on the average properties of the nuclei, such as the strength function, various widths, etc., rather than on individual resonance parameters. The study of the cross section in the kev region can therefore be expected to yield information about these average properties, rather than parameters of specific levels. While the average cross section is an important method[13] for measuring the strength function, its use for σ_p is valuable mainly in establishing that the value in the kev region is equal to that at low energy. This equality has important theoretical implications, however, in establishing the validity of the potential scattering as a cross section that is constant with energy. Thus, once "nearby" resonances are subtracted, the cross section is constant and the present work shows that constancy is attained after removal of the effect of only a small number of resonances, of the order of 5 to 10.

The transmission *vs* flight-time curve averaged over resonances has a slope that for thin samples is proportional to the strength function, Γ_n^0/D, and can be used[13] for its accurate determination. Although the intercept of the curve at zero flight time gives the potential scattering, the transmission is too near unity for accurate results. For a thick sample, on the other hand, the average transmission is

$$T_{Av}=T_p\left[1-2\sqrt{2}\pi\lambda\!\!\!^{-}\frac{\Gamma_n}{D}\sqrt{n}\right], \tag{13}$$

if we assume that $g\approx\frac{1}{2}$, that $\Gamma\approx\Gamma_n$ in the kev region, and that interference terms cancel. Here T_p is the transmission corresponding to σ_p alone, D is the average spacing for levels of a single spin state, and n is the sample thickness. From Eq. (13), by neglecting second and higher powers of (Γ_n/D), we get

$$(d/dn)(\log T_{Av})=[\sigma_p+\sqrt{2}\pi(\lambda\!\!\!^{-}/\sqrt{n})(\Gamma_n/D)]. \tag{14}$$

This equation shows that for very thin samples the slope is much greater than σ_p, because the resonances are also effective in selectively removing the neutrons from the beam and therefore lowering the average transmission. However, as the sample thickness increases, the beam get improverished in the neutrons of the resonant energies, and after a certain thickness of the sample, the slope of $(d/dn)(\log T_{Av})$ is essentially equal to σ_p.

In deriving Eq. (13) it was assumed that the areas due to negative and positive interference between resonance and potential scattering are equal and can be neglected. While the equality always holds for cross sections, it is only true for a thin sample when the average transmission curve is being considered. Because of the nonlinear relationship between transmission and cross section ($T=e^{-n\sigma}$), for thick samples the average transmission curve has a slope that corresponds to a cross section less than σ_p. This "hardening" of the beam is clearly illustrated by the curves of Fig. 3, and it definitely must be taken into account in obtaining σ_p from the thick-sample transmission curve, rather than a simple application of Eq. (14).

In order to test the validity of the above considerations, four elements, Ag, Ta, Th, and U, were experimentally investigated, and in each case the experimental transmissions for thick samples were compared with computed curves based on the known average resonance parameters. In order to take hardening into effect accurately, detailed transmission curves were calculated for typical resonances, rather than by use of Eq. (14). In the computation, a typical resonance is drawn including interference effects, and this resonance is then Doppler-broadened point for point and converted to average transmissions for various values of sample thickness. Computed transmissions for tantalum obtained in this way are shown in Fig. 3 for various single values of Γ_n, as well as for a weighted distribution of Γ_n's corresponding to that actually observed.[10] The experimental points agree best with the curve based on the distribution of Γ_n's. The departure of points at low transmission from the theoretical curve may result from uncertainty in the background, which affects low values of T markedly.

For each of the other elements, only a single Γ_n (the average for the element) was used in the computations, because, as Fig. 3 shows, while the absolute value of the average transmission changes with the

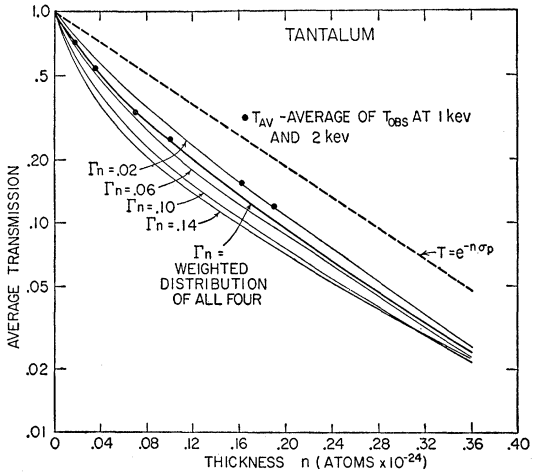

FIG. 3. The measured transmissions for thick samples of tantalum in the kev energy region. The calculated curves are based on a potential scattering cross section of 8.5 barns and various assumed values of neutron widths.

[13] D. J. Hughes and V. E. Pilcher, Phys. Rev. **100**, 1249(A) (1955); Schwartz, Pilcher, Hughes, and Zimmerman, Bull. Am. Phys. Soc. Ser. II, **1**, 347 (1956).

Γ_n assumed, the slope is affected only slightly by the choice of Γ_n. Figure 4, for normal silver, illustrates how this behavior is utilized in practice. Here the value of Γ_n chosen for the computed transmission is too small, but the value of σ_p used in the computation 6.2 b, is correct for the computed transmission because the computed curve has a slope in agreement with experiment. In order to estimate the error in σ_p determined by this method, transmission curves were also computed for slightly different values of σ_p and compared with the experimental points, resulting in an error for silver of ± 0.5 b.

Because of the lengthy calculations involved and the difficulty in measuring low transmissions, the average-cross-section method was used only for the four elements listed. However, the verification in the kev region of the values of σ_p obtained at low energy is a valuable confirmation and, in addition, helps to establish the validity of the concepts of potential scattering as constant with energy, regardless of the fluctuating resonance structure.

III. EXPERIMENTAL RESULTS

The measurements of potential scattering reported here were made for normal isotopic mixtures of each element. For all cases the between-resonances method was used and for four elements, silver, tantalum, thorium, and uranium, the potential scattering was also measured by the average-cross-section method. In Table I the results of all the determinations are summarized. Wherever the measurements were made by both methods, the weighted average is quoted in the table. Where the contribution of resonances was not large, σ_p could be measured to about 2%, or 1% in R', but the error is several times larger where the correction for resonances is large. The measured potential scattering is listed for each element and the value of R' obtained from the relation $\sigma_p = 4\pi(R')^2$. The values of R, the radius of the nuclear potential well, listed in Table I will be discussed later. They are the radii obtained from R' by utilizing the theoretical

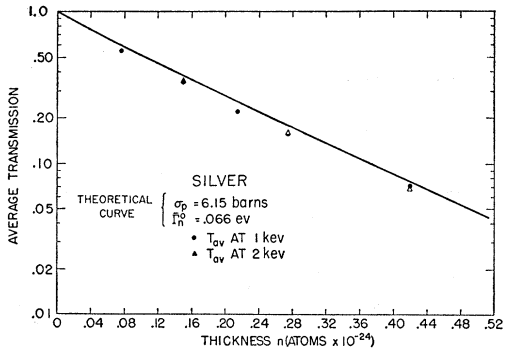

FIG. 4. The measured transmission as a function of sample thickness for silver in the kev region compared with the theoretical curve calculated for the constants shown.

TABLE I. Summary of the experimental results. The values of R' are obtained from the measured σ_p by the relation $\sigma_p = 4\pi(R')^2$ and the radii R are calculated by use of the theoretical R'/R ratios.

Element	Group	A	$A^{\frac{1}{3}}$	σ_p (barns)	R' (10^{-13} cm)	R (spherical nuclei) (10^{-13} cm)	R (deformed nuclei) (10^{-13} cm)
Copper	I	63.5	3.99	6.8±0.5	7.4±0.3	4.8±0.2	
Zinc	II	65.4	4.03	5.7±0.3	6.7±0.2	4.4±0.1	
Yttrium	II	88.9	4.46	5.7±0.2	6.7±0.1	5.7±0.1	
Zirconium	I	91.2	4.50	6.3±0.3	7.1±0.2	6.2±0.2	
Niobium	I	92.3	4.52	6.2±0.2	7.0±0.1	6.2±0.1	
Molybdenum	I	96.0	4.58	5.8±0.1	6.8±0.1	6.1±0.1	
Silver	I	107.9	4.76	5.7±0.4	6.7±0.2	6.6±0.2	
Tin	I	118.7	4.92	4.4±0.1	5.9±0.1	6.1±0.1	
Barium	I	137.4	5.16	4.3±1.0	5.8±0.6	7.0±0.8	7.4±0.8
Neodymium	II	144.3	5.25	5.0±0.6	6.3±0.4	7.5±0.4	8.6±0.5
Tantalum	I	181.0	5.66	8.5±0.8	8.2±0.4	6.3±0.3	8.6±0.3
Gold	I	197.0	5.82	11.2±0.3	9.4±0.1	7.7±0.1	8.0±0.1
Thallium	II	204.4	5.89	11.5±0.8	9.6±0.3	8.0±0.3	8.3±0.3
Lead	II	207.2	5.92	11.3±0.5	9.5±0.2	8.0±0.2	8.3±0.2
Bismuth	I	209.0	5.93	10.2±0.2	9.0±0.1	7.7±0.1	7.8±0.1
Thorium	II	232.0	6.15	12.0±0.3	9.8±0.1	8.9±0.1	8.8±0.1
Uranium	I	238.1	6.20	10.7±0.3	9.2±0.1	8.6±0.1	8.4±0.1

treatments of Feshbach, Porter, and Weisskopf,[3] and of Chase, Wilets, and Edmonds.[5]

Some of the results of Table I deserve particular mention and these will now be considered. For the purpose of brevity in this presentation, the elements investigated are divided into two groups: (I), those in which the negative energy levels did not affect the results of the between-resonances method significantly, and (II), those in which the negative levels resulted in significant corrections. In general, the results are not comparable with previous measurements of potential scattering in the resonance region because, in former analyses, usually only a single resonance was subtracted from the total cross section, the remainder being considered the potential scattering.

Group I

In this group of nuclei, as already discussed, parameters of negative energy levels are assigned only to establish that a level of average strength can remove any discrepancy in σ_{abs} at thermal. In Group I, the negative levels have no effect on the measured σ_p, hence no special significance was attached to their energy assignments, and we shall not consider them in detail. Thus zirconium, niobium, molybdenum, silver, tin, and barium all have thermal absorption cross sections that are greater than can be accounted for by the known resonances. In each of these cases, however, it was possible to account for the discrepancy in terms of a level of reduced neutron width equal to Γ_n^0, the average value for the element, located at a reasonable negative energy. For the other elements of Group I, copper, tantalum, gold, bismuth, and uranium, the resonances at positive energy accounted completely for the thermal absorption cross section, so no negative energy levels were necessary. For gold, a hitherto unreported resonance was found at 46.5 ev with a Γ_n^0 of 2.0×10^{-5} ev.

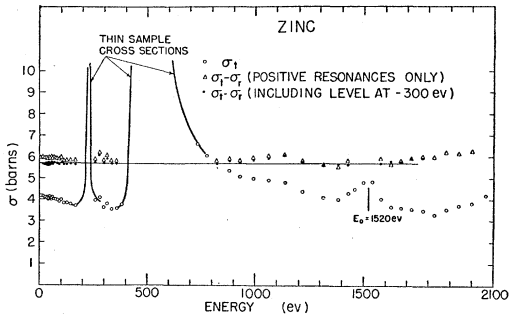

FIG. 5. The determination of the potential scattering for zinc by the between-resonances method; inclusion of a level at −300 ev accounts for the thermal absorption cross section and produces a constant $\sigma_t-\sigma_r$, giving a potential scattering of 5.7±0.3 barns.

Group II

For these elements, negative energy levels have sufficient strength so that they must be taken into account in the potential-scattering determination. Because of the greater importance of the negative energy levels relative to those of Group I, we shall briefly consider each case individually.

Zinc.—A thick sample of zinc (0.435×10^{24} atoms/cm^2), run in the energy interval 10 ev to 2000 ev, yielded the total cross section shown in Fig. 5. After correction for the known positive energy levels, the $(\sigma_t-\sigma_r)$ revealed an energy variation below 400 ev. Also, of the measured σ_{abs} of 1.06±0.05 barns only 0.61 barn was accounted for by the known levels. It was found that a level at $E_0=-300$ ev with $g\Gamma_n^0=0.023$ ev accounted for the discrepancy in σ_{abs} and the slope in $(\sigma_t-\sigma_r)$, Fig. 5, within the limits of the experimental accuracy.

Yttrium.—The measured cross section showed no resonances in the region of observation from a few ev to 2 kev. Nevertheless, the cross section decreased with increasing energy, strongly indicative of the presence of a nearby negative energy level. The observed cross section was corrected for the four known resonances between 2 and 12 kev, and the resulting shape was fitted to a single-level Breit-Wigner formula for the negative energy level. The resulting parameters for the resonance are: $E_0=-300$ ev and $g\Gamma_n=0.13$ ev. These parameters, chosen to give a constant $\sigma_t-\sigma_r$, were found to account for the thermal absorption cross section, only a negligible part of which can be attributed to the positive levels.

Thallium.—Two thick samples ($n=0.0697$ and 0.2082×10^{24} atoms/cm^2) of thallium were run at 6000 and 10 000 rpm, respectively. As Fig. 6 shows, excellent agreement was observed in the data for the two different thicknesses. Out of the known $\sigma_{abs}=3.3\pm0.5$ barns, only 0.5 barn is accounted for by the known levels. Estimation of the parameters of the negative energy level is rendered extremely difficult because of insufficient knowledge of the parameters of the positive energy levels. An area analysis of the observed resonance at $E_0=1108$ ev was made, and $fg\Gamma_n^0=0.34$ ev was obtained, where f is the unknown abundance of the responsible isotope. It was estimated that a resonance at $E_0=-40$ ev, with $fg\Gamma_n^0=0.14$ ev, accounts for the discrepancy in σ_{abs}, but uncertainty in the location of this level increases the final error in the potential scattering.

Lead.—A thick sample ($n=0.158\times10^{24}$ atoms/cm^2) of lead was run in the energy region 250 ev to 10 kev, and no resonances were observed. Existing data[14] on the 46.5-kev resonance in Pb^{207} were analyzed, on the assumption that $\Gamma_\gamma=3$ ev[15], giving $g\Gamma_n=3$ ev. Corrections to the total cross sections were applied for this resonance alone, as the contribution of higher energy resonances would be canceled by the approximately equal and opposite contribution of negative energy resonances. Of the measured $\sigma_{abs}=0.17$ barn, only 0.02 barn is accounted for by the known levels, and the rest must be attributed to a negative energy level. Since little is known concerning the parameters of the resonances in lead, the assignment of the negative energy level is rendered very difficult. Depending on whether this level is at −1 kev or −10 kev, its contribution to σ_t, in the region of energy observed, would be 0.07 barn or 0.7 barn. This uncertainty is reflected in the quoted error of the final value of σ_p in Table I.

Thorium.—The determination of σ_p by the between-resonances method has already been discussed in connection with the explanation of the method in Sec. II. There it was found that a level at −7 ev with $g\Gamma_n^0=5.5\times10^{-3}$ ev removed the discrepancy in σ_{abs} and produced a constant $\sigma_t-\sigma_r$. Four different thicknesses of thorium were also run for the average cross-section method in the kev energy region, with a resulting σ_p of 12.2±0.8 b compared with the 12.0±0.3 b of the between-resonances method. Although the latter value

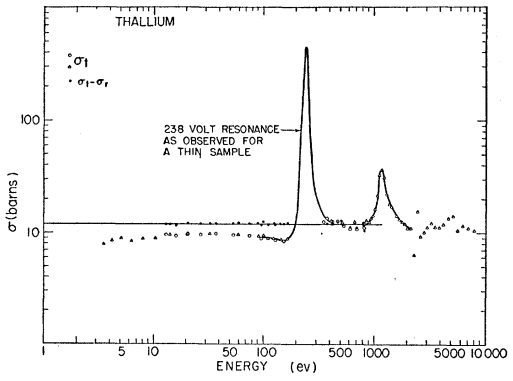

FIG. 6. The determination of the potential scattering of thallium by the between-resonances method. A negative energy level is necessary to account for the thermal absorption but it produces no significant effect on $\sigma_t-\sigma_r$, which gives $\sigma_p=11.5\pm0.8$ barns.

[14] Newson, Gibbons, Marshak, Williamson, Mobley, Toller, and Block, Phys. Rev. **102**, 1580 (1956).
[15] A. G. W. Cameron, Can. J. Phys. **35**, 666 (1957).

is more accurate, the averaging method helps to establish the constancy of potential scattering over energy ranges covering many resonances.

Neodymium.—Two thick samples ($n=0.145$ and 0.072×10^{24} atoms/cm^2) were run in the energy region 0.5 ev to 70 ev. The cross section, Fig. 7, exhibits a strong $1/v$ component, suggesting a negative energy level, and there is also a large σ_{abs} discrepancy. The discrepancy in thermal cross section can be removed by a resonance at $E_0=-14$ ev, with $fg\Gamma_n^0=0.021$ ev, where f denotes the isotopic abundance. It is seen in Fig. 7 that there is a slight departure from constancy of $(\sigma_t-\sigma_r)$ in the region 0 to 5 ev, even after taking the resonance at -14 ev into account. This result indicates that another small negative energy resonance exists near zero energy. However, it does not materially affect $\sigma_t-\sigma_r$ in the region above 5 ev, which is the basis for the final value of σ_p.

IV. CONCLUSIONS

Because the present results cover a wide range of atomic weights, it is possible to obtain from them the radius of the nuclear potential well with little dependence on model details, and to use the same information to check the predictions of the various optical models. Table I contains, in addition to the measured values of R', the nuclear radii R resulting from the theoretical (R'/R) ratios given by Feshbach, Porter, and Weisskopf[3] (spherical nuclei), and by Chase, Wilets, and Edmonds[5] (deformed nuclei). Since the latter computed R'/R for $A>130$ only, no results for R are shown at lower A based on their calculations. The potential radii thus obtained are about the same for both models for nuclei of small deformation but differ widely for values of A corresponding to large deformations. In order to determine R from the measurements, as well as to investigate the details of the model predictions, it is necessary to consider the variation of R' and R with atomic weight.

In Fig. 8 are plotted the measured values of R' as a function of A, as well as the computed curves of

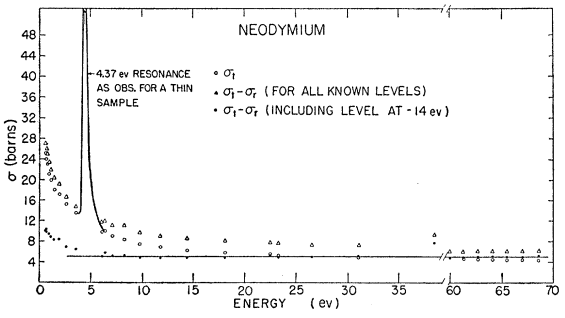

FIG. 7. The determination of the potential scattering of neodymium by the between-resonances method. A single negative energy resonance is assumed to account for the thermal absorption; this level produces a constant $\sigma_t-\sigma_r$ except for the lowest energies, implying that a second negative energy resonance near zero probably exists.

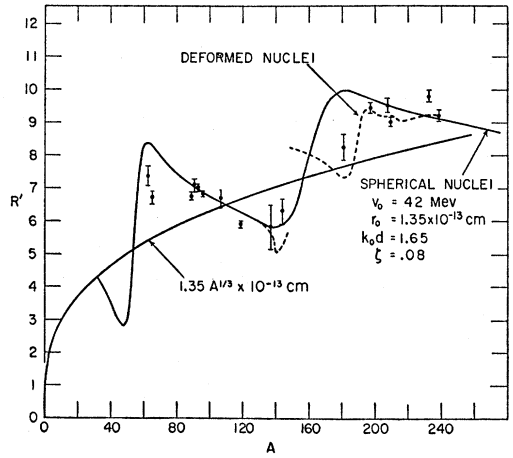

FIG. 8. Comparison of the experimental values of R' (in units of 10^{-13} cm) with the predictions of optical nuclear models. The constants shown are for the calculations of Feshbach, Porter, and Weisskopf for spherical nuclei and the dashed line corresponds to the calculations of Chase, Wilets, and Edmonds for deformed nuclei.

Feshbach *et al.*[3] and Chase *et al.*[5] The theoretical curves give R' for the R shown, $1.35\,A^{\frac{1}{3}}\times10^{-13}$ cm. The optical-model parameters quoted in Fig. 8 are those of the spherical model of Feshbach *et al.*[3] Chase *et al.*[5] used a model in which the absorption, or imaginary component, is confined to the nuclear surface, and the asphericity corresponds to the known quadrupole moments. The general validity of the semitransparent nucleus is immediately obvious because the measured points do not correspond to the $1.35\,A^{\frac{1}{3}}$ curve, as they would for a "black" nucleus for which $\sigma_p=4\pi R^2$.

In the region $A=90-130$, where nuclei are nearly spherical, it is seen that the agreement between the theoretical curve and the experimental data is very good. From $A=130$ to 190, the experimental points are in considerable disagreement with the theoretical curve of Feshbach *et al.*, based on spherical nuclei. As it is in just this region of A that the nuclei are considerably deformed, a better qualitative agreement with the curve of Chase *et al.* is therefore to be expected. It is seen that the more complicated nature of the latter curve agrees with the experimental points in general. Perhaps some change in the rather arbitrary parameters assumed in the calculation for aspherical nuclei will improve the agreement.

Thus the general trend with A of the measured values of R', and in particular for A's of high deformation, serves as a verification and test of the optical models. In addition, the nuclear potential radius can be obtained from R', with the most certainty for nuclei of small deformation, for which the dependence on the details of the model is small. In addition, as already pointed out, the values of A where $R'=R$ are particularly suited for radius determination, because these A's are fixed essentially by VR^2, and the latter values are established separately, by the strength function

results,[13] independent of the present measurements. Thus the measurements for A's in the range 90–130 and 210–240 can be used to obtain R with only slight uncertainty arising from the optical-model parameters. The radius shown in Fig. 8 is given by $R=r_0A^{\frac{1}{3}}$ with $r_0=1.35\times10^{-13}$ cm. It is felt that the present results fix r_0 as

$$r_0=(1.35\pm0.04)\times10^{-13}\text{ cm},$$

considering both experimental errors as well as the slight model dependence. The accuracy of the results is not sufficient to rule out an alternative form of the radius formula sometimes used, which includes a constant of the order of 10^{-13} cm, but there is no need for such a constant in fitting the results.

Nuclear potential radius determinations have recently been made by a number of proton-scattering experiments analyzed[1] on the basis of the optical model. The measured angular distributions have usually been interpreted in terms of an r_0 about 1.2×10^{-13} cm, but it has become clear more recently that the r_0 obtained depends critically on the potential depth assumed. Actually, proton-scattering experiments in the range 1 to 100 Mev determine the product VR^n, where $n=2$ at low energies and may be as large as 3 at energies of the order of 100 Mev. In the analysis there is a large amount of arbitrariness in breaking the product into V and R. However, the range of r_0 that is consistent with the proton scattering, even though not accurately fixed, seems to be about $(1.2-1.3)\times10^{-13}$ cm and thus in reasonable agreement with the present value of 1.35×10^{-13} cm. As the well depth is different for protons and neutrons it is not possible to use the depth determined from neutron scattering, 42 Mev, to aid in analysis of the proton experiments.

In contrast to the present results on the nuclear potential radius, measurements[16] on the nuclear charge radius by scattering of high-energy electrons lead to

$$r_0=1.09\times10^{-13}\text{ cm}$$

for heavy elements. Here $r_0A^{\frac{1}{3}}$ is the distance to the halfway point of the charge distribution, similar to the R of our Eq. (4), which is the distance to the halfway point of the potential distribution. (Reference 16 uses the notation $r_1A^{\frac{1}{3}}$ for this distance to the halfway point.)

We thus have conclusive evidence of a large difference between the nuclear potential and charge radii, which is

$$(1.35-1.09)\times10^{-13}=0.26\times10^{-13}\text{ cm}$$

if expressed in terms of the parameter r_0. As already mentioned, the present results do not cover a sufficiently large range of A to determine accurately the functional dependence of R on A. In terms of a particular nucleus, gold ($A^{\frac{1}{3}}=5.82$), the radius of the potential is larger than that of the charge distribution by 1.5×10^{-13} cm. The possibility that this result is caused by a further extent of neutrons than protons in the nucleus[17] now seems to be eliminated, for recent π-meson scattering measurements[18] indicate that protons and neutrons in the nucleus have the same extent. The difference is probably to be ascribed to the range of nuclear forces,[19,20] which enables the incoming neutron to be affected by the neutrons and protons in the nucleus before it reaches the actual nuclear surface. This explanation would lead one to expect a variation of R with A somewhat different for potential and charge. Extension of the present measurements to lower A might help to reveal this difference.

Drell and Williams[21] have recently suggested that the effect of the nuclear force range should decrease at relativistic energies and that as a result the potential radius should approach the nuclear charge radius for incident protons or neutrons of several Bev energy. No clear-cut measurements of the nuclear potential radius by elastic scattering are available as yet in the energy region of interest, however.

[16] Reviewed by R. Hofstadter, Revs. Modern Phys. **28**, 214 (1956).

[17] M. H. Johnson and E. Teller, Phys. Rev. **93**, 357 (1954).
[18] Abashian, Cool, and Cronin, Phys. Rev. **104**, 855 (1956).
[19] S. D. Drell, Phys. Rev. **100**, 97 (1955).
[20] K. A. Brueckner, Phys. Rev. **103**, 1121 (1956).
[21] S. D. Drell and R. W. Williams (private communication).